pISSN 2384-1095
eISSN 2384-1109

iMRI 2016;20:114-119

http://dx.doi.org/10.13104/imri.2016.20.2.114

iMRI
Investigative Magnetic Resonance Imaging

Diagnosis of Right Ventricular Vegetation on Late Gadolinium-Enhanced MR Imaging in a Pediatric Patient after Repair of a Ventricular Septal Defect

Jewon Jeong[1,2], Hae Jin Kim[2], Sung Mok Kim[2,3], June Huh[4], Ji-Hyuk Yang[5], Yeon Hyeon Choe[2,3]

[1]Department of Radiology, Soonchunhyang University Seoul Hospital, Seoul, Korea
[2]Department of Radiology, Samsung Medical Center, Sungkyunkwan University School of Medicine, Seoul, Korea
[3]HVSI Imaging Center, Heart Vascular Stroke Institute, Samsung Medical Center, Sungkyunkwan University School of Medicine, Seoul, Korea
[4]Division of Cardiology, Department of Pediatrics, Samsung Medical Center, Sungkyunkwan University School of Medicine, Seoul, Korea
[5]Department of Thoracic and Cardiovascular Surgery, Samsung Medical Center, Sungkyunkwan University School of Medicine, Seoul, Korea

Case Report

Received: April 5, 2016
Revised: May 19, 2016
Accepted: May 20, 2016

Correspondence to:
Yeon Hyeon Choe, M.D., Ph.D.
Department of Radiology and HVSI Imaging Center, Heart Vascular Stroke Institute, Samsung Medical Center, Sungkyunkwan University School of Medicine, 81 Ilwon-ro, Gangnam-gu, Seoul 06351, Korea.
Tel. +82-2-3410-2509
Fax. +82-2-3410-2559
Email: yhchoe@skku.edu

We report a case of vegetation in a 4-year-old female with infective endocarditis, diagnosed by late gadolinium-enhanced (LGE) cardiovascular magnetic resonance (CMR) imaging. The patient had a history of primary closure for ventricular septal defect and presented with mild febrile sensation. No remarkable clinical symptoms or laboratory findings were noted; however, transthoracic echocardiography demonstrated a 14 mm highly mobile homogeneous mass in the right ventricle. On LGE CMR imaging, the mass showed marginal rim enhancement, which suggested the diagnosis of vegetation rather than thrombus. The extracellular volume fraction (≥ 42%) of the lesion was higher than that of normal myocardium. Based on the patient's clinical history of congenital heart disease and pathologic confirmation of the lesion, a diagnosis of infective endocarditis with vegetation was made.

Keywords: Infective endocarditis; Vegetation; Late gadolinium enhancement; Cardiovascular magnetic resonance imaging; Right ventricle; Congenital heart disease

INTRODUCTION

The diagnosis of infective endocarditis (IE) is established on the modified Duke's criteria, including clinical presentation, laboratory findings and results of imaging modalities including echocardiography (1). Echocardiography is generally recommended as the first-line diagnostic imaging method and shows high diagnostic performance. Echocardiography, however, has several limitations in differentiating vegetation from thrombus or cardiac tumors, in cases of early stage IE and small vegetation. As recent

technical developments in computed tomography (CT) and magnetic resonance (MR) imaging can provide high-quality images and profound information (2, 3), they are expected to play important roles in diagnosis of IE. To date, however, few studies have reported the cardiovascular magnetic resonance (CMR) findings of IE and no characteristic finding of vegetation itself on CMR imaging has been reported. Here, we report a case of vegetation in the right ventricle with IE, which showed marginal rim late gadolinium-enhanced (LGE) in CMR in a patient with history of surgery for a ventricular septal defect (VSD).

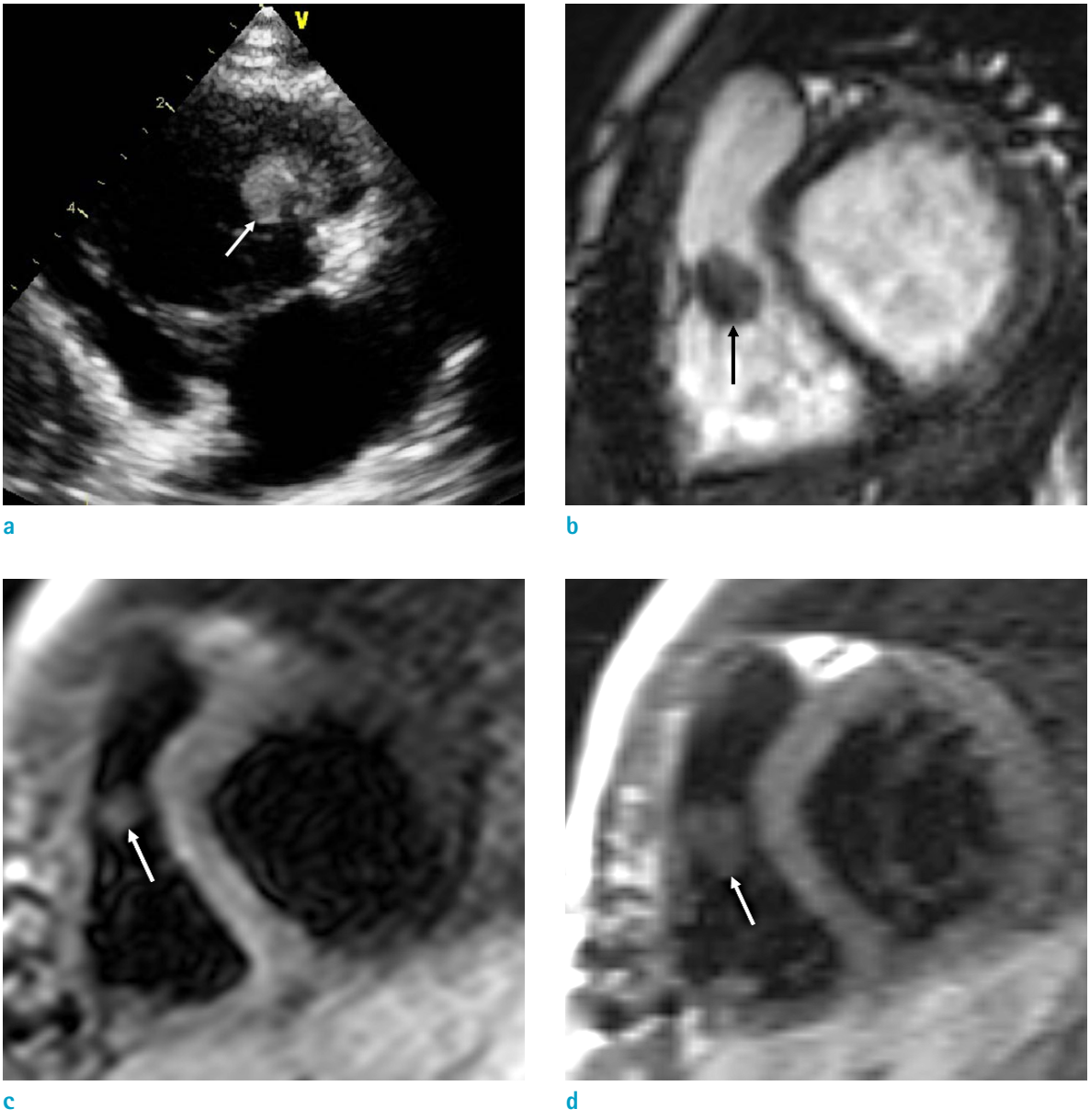

Fig. 1. A 4-year-old female with a vegetation in the right ventricle (RV). (a) Initial transthoracic echocardiography shows a14 × 11 mm-sized highly mobile homogeneous mass (arrowhead) in RV, which is attached to the ventricular septal defect primary closure site. (b-e) CMR (b), 8 days after initial the echocardiography. The mass (white arrows) is seen in the RV, attached to the anterior wall on a short-axis-view cine MR image and shows iso-signal intensity as compared with the myocardium on T2-weighted (c) and T1-weighted (d) images.

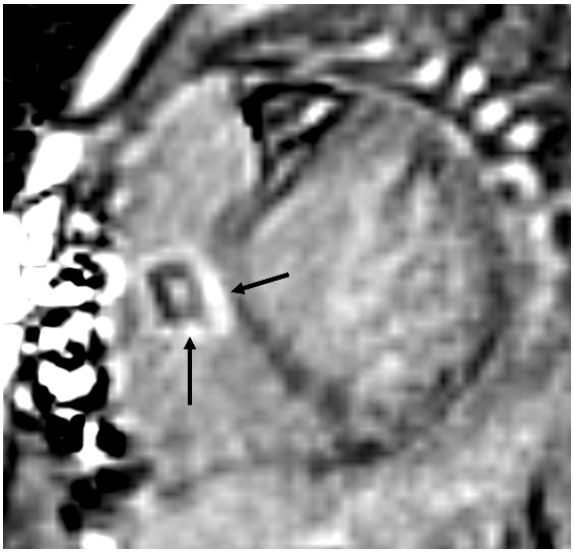

e

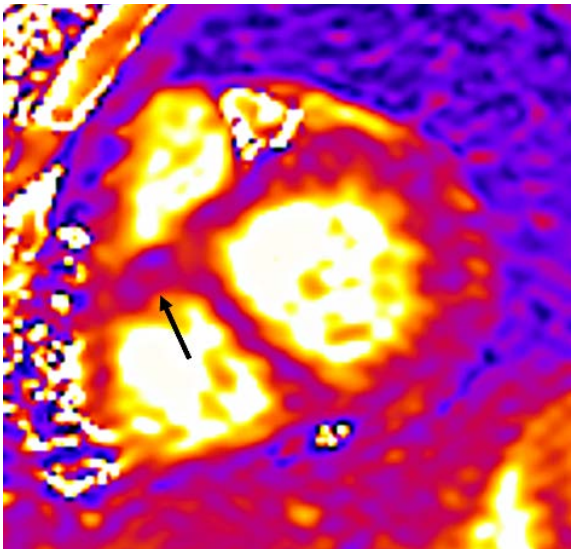

f

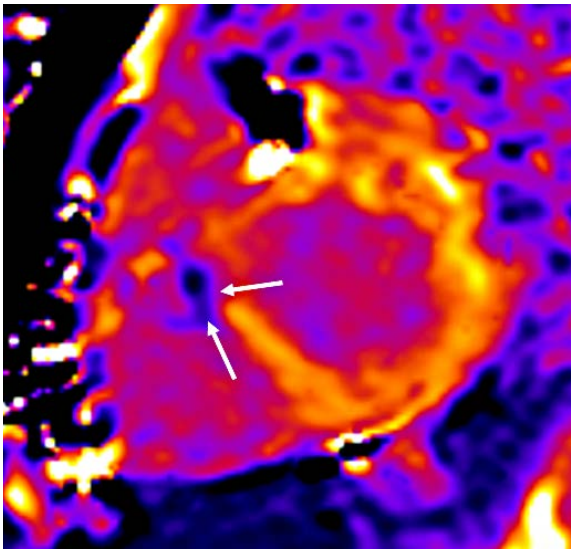

g

h

Fig. 1. Late gadolinium-enhanced image in a short-axis view (e) demonstrates marginal rim enhancements (black arrows). (f, g) A T2 map (f) and postcontrast-T1 map image (g) show that the T2 relaxation time of the lesion is similar to that of normal left ventricular myocardium and that peripheral components (arrows) of the vegetation show lower T1 values than the myocardium. (h) Resected specimen shows a soft, round, encapsulated, and whitish mass consisting of granular tissue.

CASE REPORT

A 4-year-old female with a history of perimembranous VSD and patent foramen ovale with primary closure about 10 months ago, presented to our institution with 2 weeks of mild febrile sensation. She had undergone a dental procedure for treatment of a decayed tooth about 2 months prior. Physical examination was unremarkable. Laboratory findings were within the normal range and blood cultures were negative. Her electrocardiogram was normal. Transthoracic echocardiography (TTE) revealed a 14 × 11 mm highly mobile homogeneous mass in the right ventricle (RV), which was attached to the anterior wall (Fig. 1a). Considering her clinical history of surgery for congenital heart disease and a recent dental procedure, infective endocarditis with vegetation was the most likely diagnosis.

Thus, she received antibiotic treatment on admission. After 1 week, her symptoms improved; however, follow-up TTE again showed the mass in the RV without interval size change. Clinically, thrombus or primary cardiac masses, such as a myxoma or fibroelastoma, could not be completely excluded. CMR imaging was subsequently performed to assess the mass in RV, using a 1.5-T MR scanner (Avanto 1.5T, Siemens Healthcare, Erlangen, Germany) with electrocardiographic gating. The sequences and parameters of CMR were as follows. Cine MR imaging with balanced steady-state free precession (TrueFISP) (repetition time [TR] = 3 ms, echo time [TE] = 1.41 ms; slice thickness, 6 mm; acquisition matrix, 272 × 174; short-axis view, four-chamber view, two-chamber view), T1-weighted imaging (double inversion-recovery T1-weighted image with black blood; TR = 499 ms, TE = 23 ms; slice thickness 6 mm), T2-weighted imaging (triple inversion-recovery T2 weighted image with black blood and fat suppression; TR = 1007.5 ms, TE = 64 ms; number of trigger pulse = 2; slice thickness, 6 mm; acquisition matrix, 256 × 156). Quantitative T2 mapping used three single-shot TrueFISP images with different T2 preparation times and pre-T1 mappings with a modified Look and Locker technique using a single-shot inversion recovery TrueFISP readout with a 5(3)3 scheme. Imaging data were acquired during mid-diastolic phase along the same short-axis planes as the T2-weighted images. The acquisition parameters for T2 mapping were: T2 preparation times = 0 ms, 25 ms, and 55 ms; 3 recovery heartbeats between each acquisition; TR = 2.71 ms; TE = 1.4 ms; acquisition matrix = 192 × 160; acquisition time = 7 × R-R; flip angle = 70°; and bandwidth = 916 Hz/pixel. The acquisition parameters for T1 mapping were: TR = 2.43 ms, TE = 1.01 ms, inversion time [TI] start = 110 ms; TI increment = 80 ms; flip angle = 35°, acquisition matrix = 192 × 124, field of view = 320 × 400 mm, slice number = 8 slices. Late gadolinium-enhanced imaging (phase-sensitive inversion recovery; TR = 2.83; TE = 1.23 ms; slice thickness 6 mm; acquisition matrix = 256 × 190, resolution 1.33 mm × 1.33 mm; time to inversion = 400 to 500 ms for 5 and 16 min delay after contrast injection, respectively) was performed after intravenous injection of 4 mL (0.1 mmol/kg) of gadoterate meglumine (Dotarem, Guerbet, Cedex, France). The post-T1 mapping was performed 15 min after contrast medium injection, using the same slice axis and parameters as pre-T1 mapping. T2-pixel maps and pre-post T1-pixel maps were generated after fully automated non-rigid motion correction and pixel-wise fitting at the scanner (Siemens Healthcare). The extracellular volume (ECV) fraction was calculated as follows: ECV fraction = (ΔR1 of myocardium or vegetation / ΔR1 of blood pool) × (1 - hematocrit), where R1 = 1 / T1 and ΔR1 = postcontrast R1 - precontrast R1.

On CMR images, a 10.5 × 12.6 mm ovoid mass was seen in the RV attached to the anterior wall, and caused partial obstruction of the right ventricular outflow tract. The mass showed iso-signal intensity on T2- and T1-weighted images as compared with that of the myocardium (Fig. 1b-d). Additionally, on LGE images, a marginal rim enhancement of the mass was seen (Fig. 1e). On quantitative T2 map images, the T2 relaxation time of the mass in the RV was 43 ms (Fig. 1f). The precontrast T1 value of the mass was 1087-1195 ms. On post-T1 mapping images, the mean myocardial T1 value was 433-584 ms (Fig. 1g). The patient's hematocrit was 32.8% and the ECV fraction for the mass was 42-75% according to areas with different appearances on post-contrast images. The T2 relaxation time, precontrast T1 relaxation time, postcontrast (15 min) T1 relaxation time, and ECV fraction of normal left ventricular myocardium were 47 ms, 982 ms, 639 ms, and 30%, respectively.

Surgery was performed to confirm the diagnosis and remove the mass. During the surgery, a 1 cm encapsulated mass was seen attached to the anterior wall of the RV, between the VSD closure patch and the septal leaflet of the tricuspid valve. The resected specimen revealed a soft, round, encapsulated, and whitish mass consisting of granular tissue (Fig. 1h). Pathologic findings of the resected specimen from the RV were consistent with vegetation. According to the modified Duke's criteria (1), a final diagnosis of IE was established. The postoperative course was uneventful and the patient was discharged with full recovery.

DISCUSSION

Right-sided IE is less frequent than left-sided IE and seen most frequently in intravenous drug users or patients with underlying congenital heart disease. Unrepaired VSD is closely associated with IE (4, 5). One recent study (6), however, reported that the underlying condition of pediatric patients with IE has changed from unrepaired congenital heart diseases (CHD) to postoperative or no underlying CHD. Additionally, although our patient's VSD was repaired, her risk for right-sided IE was significant because she underwent a dental procedure, which can cause for bacteremia in cases of CHD-associated IE (5).

The diagnosis of IE is based on clinical information, laboratory data including blood culture, and the results of echocardiography and other advanced imaging modalities. The diagnosis of IE remains challenging due to the wide range of clinical manifestations and low specificity of laboratory findings. The majority of patients present with fever (1, 7). Transthoracic and transesophageal echocardiography (TTE/TEE) are the first imaging modalities used in diagnosis and show high sensitivity and specificity, especially when performed in a complementary manner. TTE/TEE show limited diagnostic performance in differentiating between vegetations and thrombi or cardiac tumors, in the early stage and when the vegetation is too small for detection (2, 3). In our patient, fever was absent on physical examination. Also, all laboratory findings of the patient were within the normal range and blood culture was negative. Thus, the diagnosis of the mass-like lesion on TTE and CMR imaging in our patient was challenging.

The role of advanced imaging modalities such as three-dimensional echocardiography, CT and CMR imaging for the diagnosis of IE has not been fully evaluated (1, 3, 7). To our knowledge, moreover, the features of the vegetation itself on CMR with pathologic confirmation have not been reported. Differentiation of vegetation from thrombus can be difficult, because both are shown as masses without gadolinium contrast enhancement (8). CMR of our patient showed marginal rim enhancement on LGE images, which might facilitate differentiation of vegetations from thrombi or cardiac tumors. Other findings suggesting IE on CMR imaging are myocardial LGE indicating irreversible myocardial damage or fibrosis, LGE of the endothelial lining, or perivalvular abscess (2, 9-11).

Thrombus shows variable signal intensity depending on the age of the thrombus and generally does not enhance with gadolinium contrast material. Cardiac myxoma is predominantly located in the left atrium and shows heterogeneous signal intensity and enhancement following injection of gadolinium contrast material. Cardiac papillary fibroelastoma usually arises from the valvular endocardium and capturing meaningful images on CMR is difficult due to its small size and high mobility (8).

We used T1 and T2 mapping with ECV calculation for objective tissue characterization. Many studies have reported the usefulness of T1 and T2 mapping in the evaluation of myocardial disease. Few case reports, however, have described cardiac masses with T1 and T2 relaxation time measurement (12). Saba et al. (13) reported that the mean T1 relaxation time of the cardiac thrombus and myxoma were 1044.7 ms and 1681.6 ms, respectively. The reported value of the left ventricular ECV in a healthy population is 27 ± 3% (14).

Electrocardiography-gated multislice CT provides high-resolution anatomical information in cases of IE. The CT findings of IE are vegetation, valvular aneurysm, and perivalvular abscess (3, 4). ^{18}F-fluorodesoxyglucose (^{18}F-FDG) positron emission tomography (PET)-CT could also be helpful in the diagnosis of IE, especially in patients with prosthetic valves. An abnormal FDG uptake around a prosthetic valve indicates IE with high sensitivity (3, 7).

In summary, we report the echocardiographic and MRI findings of an RV vegetation, which was pathologically confirmed in a patient with IE, and that marginal rim LGE might be considered a characteristic CMR finding of vegetation.

REFERENCES

1. Habib G, Hoen B, Tornos P, et al. Guidelines on the prevention, diagnosis, and treatment of infective endocarditis (new version 2009): the Task Force on the Prevention, Diagnosis, and Treatment of Infective Endocarditis of the European Society of Cardiology (ESC). Endorsed by the European Society of Clinical Microbiology and Infectious Diseases (ESCMID) and the International Society of Chemotherapy (ISC) for Infection and Cancer. Eur Heart J 2009;30:2369-2413
2. Dursun M, Yilmaz S, Yilmaz E, et al. The utility of cardiac MRI in diagnosis of infective endocarditis: preliminary results. Diagn Interv Radiol 2015;21:28-33
3. Thuny F, Grisoli D, Cautela J, Riberi A, Raoult D, Habib G. Infective endocarditis: prevention, diagnosis, and management. Can J Cardiol 2014;30:1046-1057
4. Bae JM, Choe YH, Hwang HW, et al. Tumor-mimicking large vegetation attached to the tricuspid valve without predisposing factors: a case report on CT and echocardiographic findings. J Korean Soc Radiol 2015;73:269-273
5. Knirsch W, Nadal D. Infective endocarditis in congenital heart disease. Eur J Pediatr 2011;170:1111-1127
6. Elder RW, Baltimore RS. The changing epidemiology of pediatric endocarditis. Infect Dis Clin North Am 2015;29:513-524
7. Bruun NE, Habib G, Thuny F, Sogaard P. Cardiac imaging in infectious endocarditis. Eur Heart J 2014;35:624-632
8. Sparrow PJ, Kurian JB, Jones TR, Sivananthan MU. MR imaging of cardiac tumors. Radiographics 2005;25:1255-1276

9. Dursun M, Yilmaz S, Ali Sayin O, et al. A rare cause of delayed contrast enhancement on cardiac magnetic resonance imaging: infective endocarditis. J Comput Assist Tomogr 2005;29:709-711
10. Sverdlov AL, Taylor K, Elkington AG, Zeitz CJ, Beltrame JF. Images in cardiovascular medicine. Cardiac magnetic resonance imaging identifies the elusive perivalvular abscess. Circulation 2008;118:e1-3
11. Ryu SY, Kim HJ, Kim SM, Park SJ, Choe YH. Detection of perivalvular abscess with late gadolinium-enhanced MR imaging in a patient with infective endocarditis. Investig Magn Reson Imaging 2016;20:75-79
12. Germain P, El Ghannudi S, Jeung MY, et al. Native T1 mapping of the heart - a pictorial review. Clin Med Insights Cardiol 2014;8:1-11
13. Saba SG, Bandettini PW, Shanbhag SM, Spottiswoode BS, Kellman P, Arai AE. Characterization of cardiac masses with T1 mapping. J Cardiovasc Magn Reson 2015;17(Suppl 1):Q32
14. Fontana M, White SK, Banypersad SM, et al. Comparison of T1 mapping techniques for ECV quantification. Histological validation and reproducibility of ShMOLLI versus multibreath-hold T1 quantification equilibrium contrast CMR. J Cardiovasc Magn Reson 2012;14:88